Available online at www.sciencedirect.com
ScienceDirect
J. of Supercritical Fluids 40 (2007) 308–316
THE JOURNAL OF Supercritical Fluids
www.elsevier.com/locate/supflu

Controlled submicro particle formation of ampicillin by supercritical antisolvent precipitation

A. Tenorio *, M.D. Gordillo, C. Pereyra, E.J. Martínez de la Ossa

Department of Chemical Engineering, Food Technology and Environmental Technologies, Faculty of Sciences, University of Cádiz, 11510 Puerto Real, Cádiz, Spain

Received 20 December 2005; received in revised form 12 June 2006; accepted 6 July 2006

Abstract

A supercritical antisolvent (SAS) technique has been used in the precipitation of ampicillin (APC), one of the world's most widely prescribed antibiotics, to control its particle size (PS) and particle size distribution (PSD). The influences of different solvents and pressure on morphologies, PS and PSD have been investigated. Three different solvents: *N*-methylpyrrolidone (NMP), dimethylsulfoxide (DMSO), and ethyl alcohol (EtOH) have been assayed. Experimental conditions (150 bar, 313 K, 20 mg/mL and ratio of CO_2 flow rate/liquid flow rate equal to 15, on a mass basis at the process operating conditions) were kept constant throughout the course of this investigation. Through simply changing the APC–liquid solvent system we observed large variations in PS and PSD, accompanied by different particles morphologies. The APC–NMP proved to be the best system for controlling the precipitation of ampicillin; both compact particles and spherical microparticles (mean diameter = 0.26 μm and standard deviation = 0.08 μm) were obtained. In a second study, ampicillin has been successfully processed in the range of 80–150 bar using NMP as liquid solvent under constant experimental conditions. A change from 80 to 100 bar led to a large reduction of the mean PS and PSD, and no significant differences were found at pressures higher than 100 bar. Conversely, an increase in pressure produced better sphericity in particle shape.

Keywords: Supercritical antisolvent; Ampicillin; Drug; Precipitation; Particle size

1. Introduction

The utilization of supercritical fluids in the processing of pharmaceutical compounds has become important in recent years [1].

Advantages such as high purity products, environmental protection, and greater experimental versatility are significant and all combine to create a viable alternative to certain conventional processing currently used in the pharmaceutical industry [2].

In fact, the content of residual solvent permitted for the final product, controlled by international safety regulations, is generally restricted to a few ppm [3] and microparticles for aerosol administration (particle sizes between 1 and 5 μm) are especially difficult to obtain by traditional micronization techniques [4,5].

The supercritical antisolvent process (SAS) uses both the high power of supercritical fluids to dissolve the organic solvents and the low solubility of the pharmaceutical compounds in supercritical fluids [6] to cause the precipitation of such compounds once they are dissolved in the organic phase.

The dissolution of the supercritical fluid into the organic solvent is accompanied by a large volume expansion and, consequently, a reduction of the liquid density, and therefore, of its solvent power, causing a sharp rise in the supersaturation within the liquid mixture. Because of the high and uniform degree of supersaturation, small particles with a narrow particle size distribution are expected [7].

Furthermore, antibiotics can be entrapped in nanoparticles of various formulations using supercritical antisolvent process. In particular, polymeric micro- and nano-particles have been found successful in the preparation of sustained drug delivery systems, hence they display enhanced therapeutic performance compared to traditional formulations [8–10].

Supercritical fluid techniques have been widely used to produce a large variety of pharmaceutical compounds, and microparticles with controlled diameter and particle size distribution have been obtained: fluticasone-17-propionate (anti-inflammatory drug) [11], nifedipine (calcium-channel blockers), felodipine and fenofibrate (hypolipidermic agent) [12], griseo-

* Corresponding author. Tel.: +34 956016458; fax: +34 956016411.
E-mail address: alvaro.tenorio@uca.es (A. Tenorio).

0896-8446/$ – see front matter © 2006 Elsevier B.V. All rights reserved.
doi:10.1016/j.supflu.2006.07.003

fulvin [5,13], ampicillin, amoxicillin and tetracycline (antibiotics) [5,14,15], lysozyme [16], salbutamol [4], acetaminophen (paracetamol) [17], β-sitosterol [13], hydrocortisone [18], rifampicin [19], carbamazepine [20], artemisinin [21], ibuprofen [22], terbutaline [23], sulfamethizole [24], insulin [25], budesonide and flunisolide (glucocorticoids) [26], erythromycin [27], budesonide (powder inhaler) [28], terbutaline sulphate (powder for pulmonary delivery) [29], cefonicid [30], salicylamide [31], theophylline [32], human growth hormone [33], felodipine [34].

Ampicillin is one of the most widely prescribed antibiotics. It is considered a penicillin and is a close relative of another penicillin, amoxicillin. Unlike penicillin, ampicillin and amoxicillin can penetrate and inhibit bacterial cell-wall synthesis (peptidoglycan cross-linking) by inactivating transpectidases on the inner surface of the bacterial cell membrane. Ampicillin is used mainly to treat infections of the middle ear, sinuses, bladder, kidney, and uncomplicated gonorrhea. It also is used intravenously to treat meningitis and other serious infections.

Using controlled-sized microparticles of ampicillin it is possible to increase its bioavailability and decrease its therapeutic dosage (thus improving efficiency). It is also possible to change its drug delivery system (transdermal, tracheobronchial and pulmonary delivery systems) by eliminating undesired secondary effect as a result of oral consumption of this pharmaceutical compound [1].

Owing to the lack of general rules that lead to successful precipitation, each solute–solvent–antisolvent system has to be studied separately, searching for the optimum solvent and experimental conditions to make SAS processing feasible.

For this reason, in this work, the precipitation of ampicillin using carbon dioxide as antisolvent has been studied and the influence of solvent and experimental pressure on morphology, PS and PSD have been investigated using SAS 200 equipment. In an initial study, three different solvents: *N*-methylpyrrolidone (NMP), dimethylsulfoxide (DMSO), and ethyl alcohol (EtOH) have been used. Experimental conditions (150 bar, 313 K, 20 mg/mL and ratio of CO_2 flow rate/liquid flow rate equal to 15, on a mass basis at the process operating conditions) were kept constant throughout the course of this investigation and were selected taking as a basis some previous studies found in the bibliography [5,14]. In a second study, ampicillin has been processed in the range of 80–150 bar, under constant experimental conditions (313 K, 20 mg/mL and ratio of CO_2 flow rate/liquid flow rate equal to 15, on a mass basis at the process operating conditions).

2. Experimental

2.1. Experimental equipment and procedures

A schematic diagram of the pilot plant, developed by Thar Technologies® (model SAS 200), is shown in Fig. 1. This equipment has been validated by performing various experiments of supercritical antisolvent precipitation of amoxicillin (AMC) before being used for supercritical antisolvent precipitation of ampicillin. The SAS 200 system is made up of the follow components: two high pressure pumps, one for the CO_2 (P1) and the other for the solution (P2), which incorporate a low dead

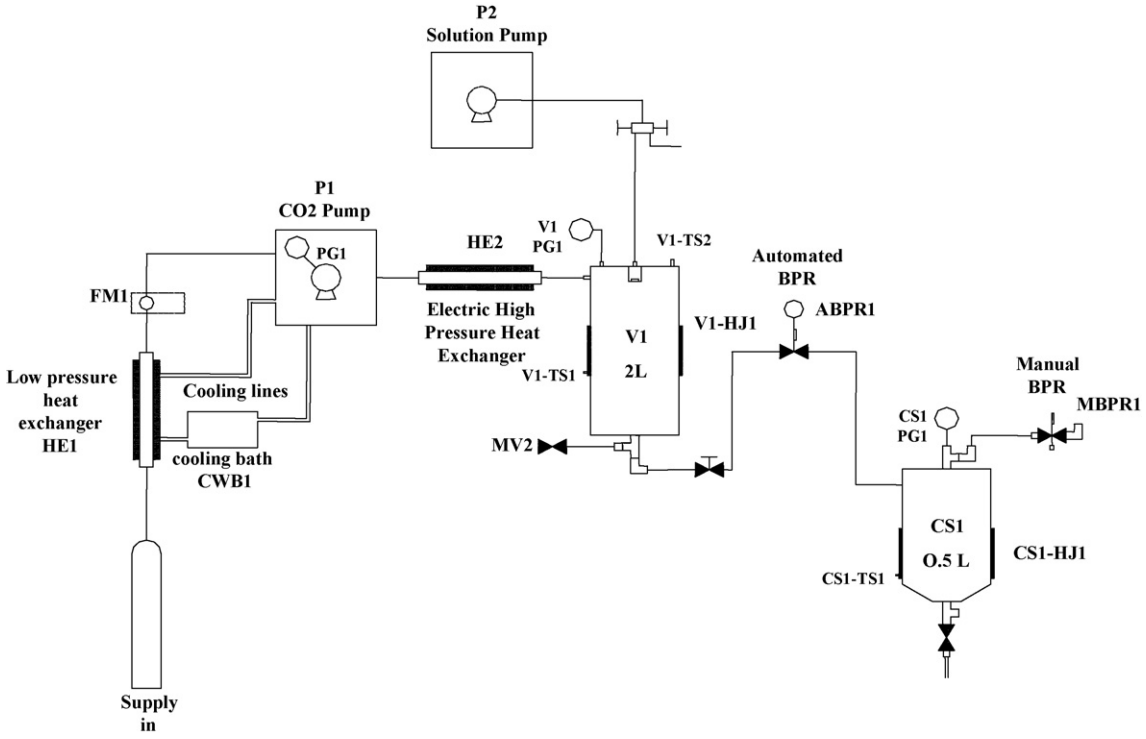

Fig. 1. Schematic diagram of the pilot plant.

volume head and check valves to provide efficient pumping of CO_2 and many types of solvent; a stainless steel precipitator vessel (V1) with 2 L volume, consisting of two parts, the main body and the frit; it also has an electric heating jacket (V1–HJ1); an automated back pressure regulator (ABPR1) of high precision attached to a motor controller with a position indicator; a jacketed (CS1–HJ1) stainless steel cyclone separator (CS1) with 0.5 L volume to separate the solvent and CO_2, once the pressure is released by the manual back pressure regulator (MBPR1). Auxiliary elements are necessary too, such as: a low pressure heat exchanger (HE1); cooling lines and cooling bath (CWB1) to keep the CO_2 inlet pump cold and to chill the pump heads. An electric high pressure heat exchanger (HE2) is used to preheat the CO_2 to bring the temperature in the precipitator vessel to the required level rapidly; safety devices (rupture discs and safety valve MV2) are included; pressure gauges measure the pump outlet pressure (P1, PG1), the precipitator vessel pressure (V1, PG1) and cyclone separator pressure (CS1, PG1) and continuous temperature measurements are made by means of thermocouples placed inside (V1–TS2) and outside (V1–TS1) the precipitator vessel, inside the cyclone separator (CS1–TS1) and on the electric high pressure heat exchanger; a FlexCOR™ coriolis mass flowmeter (FM1) is used to measure CO_2 mass flow rate and other parameters such as total mass, density, temperature, volumetric flowrate, and total volume. All parameters that influence in the precipitation process (temperature, flow rate, pressure) can be controlled either manually or automatically (using ICM software).

An important component of the SAS 200 equipment is the nozzle that sprays the liquid solution inside the precipitator vessel. A commercial stainless steel nozzle from Thar Technologies® with inner diameter of 100 μm and an *L/D* ratio of 72.5 was employed in this work. Supercritical CO_2 was delivered from another inlet point located on the top of the vessel.

All the experiments were performed following the same procedure: first of all, the CO_2 is pumped into the vessel at the same time as the electrical heater, heat exchanger and automatic back pressure regulator are switched on. When the CO_2 supercritical conditions (pressure and temperature) are achieved and the solution pump is primed, the liquid solution is pumped to the precipitator vessel and sprayed inside the vessel itself by means of the nozzle. The small drops of solvent are dissolved by supercritical CO_2 causing supersaturation of the liquid solution and the consequent precipitation of the ampicillin in the form of a powder that accumulates on the frit located at the bottom of the vessel, as well as being deposited on the internal wall of the vessel. The precipitation process finishes when the desired amount of liquid solution has been fed into the system, then the liquid pump is turned off and the supercritical CO_2 continues flowing through the precipitator vessel to remove the residual content of the liquid solvent solubilized into the supercritical antisolvent. The washing stage lasts approximately 3 h (roughly equivalent to 1.5 times the volume of the precipitator vessel) [35]. After that the supercritical CO_2 flow is stopped and the system is depressurized down to atmospheric pressure. Finally, all the precipitate is recovered from both the wall and the frit of the precipitator vessel; the analyses required, such as scanning electron microscope (SEM) and X-ray diffraction (XRD), are then carried out.

2.2. Materials and analytical methods

1-Methyl-2-pyrrolidone (NMP) (purity 99.5%), dimethyl sulfoxide (DMSO) (purity ≥99.5%) were purchased from Sigma–Aldrich Chemical (Spain). Ethanol (EtOH) and methanol (MeOH) (purity ≥99.5%) were purchased from Panreac Química (Spain). CO_2 with a minimum purity of 99.8% was supplied by Carburos Metálicos S.A. (Spain). Ampicillin sodium salt (minimum purity 91.0%) and amoxicillin (AMC) (purity ≥97%) were purchased from Sigma–Aldrich Chemical (Spain) and were used in the precipitation experiments. The ampicillin was soluble in the solvents used for the fixed experimental concentration at room temperature. A SEM picture of ampicillin as received is shown in Fig. 2.

Samples of the powder precipitated both on the vessel wall and in the frit were observed using a Quanta 200 scanning electron microscopy (SEM). Previously, the samples were put onto carbon tape and then were covered with a gold coating using a sputter coater. The SEM images were processed using Scion image analysis software (Scion Corporation) to obtain the particle sizes. After that, the mean particle size (PS), particle size distribution (PSD) and standard deviation (S.D.) were calculated using Statgraphics plus 5.1 software. More than 200 particles were counted to carry out the analysis in each experiment. X-ray diffraction pattern analysis was performed in this work to determine the possible changes in the physical characteristics of the precipitate obtained by the SAS process.

2.3. Validation of SAS 200 equipment

The correct functioning of the SAS equipment was checked by taking the amoxicillin precipitation experiments performed

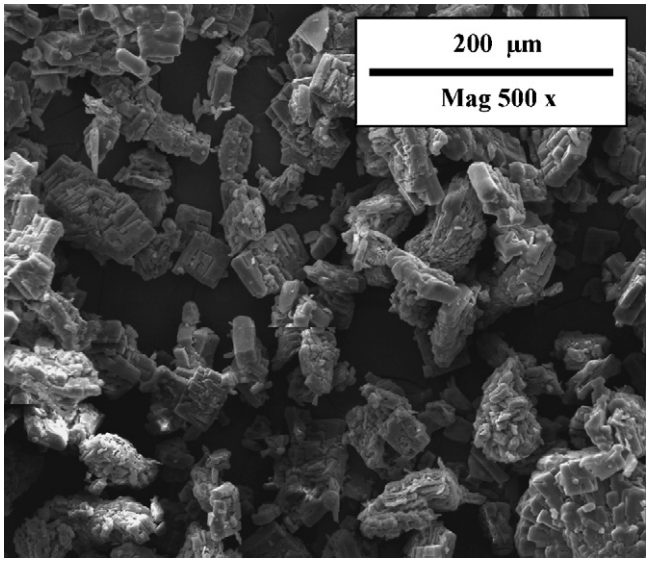

Fig. 2. SEM image of unprocessed ampicillin.

by Reverchon et al. [14] as a starting point, so the amoxicillin was precipitated varying the concentration of the AMC/NMP solution between 20 and 100 mg/mL under constant experimental conditions (150 bar, 313 K, 1 mL/min solution flow rate and 33 g/min CO_2 flow rate). Both an increase of the mean particle size and a broadening of the particle size distribution were observed with the increase of the concentration of the AMC/NMP solution. This effect can be seen qualitatively in Fig. 3a and b, where the SEM images of the amoxicillin microparticles are shown for the experiments performed operating at 20 and 100 mg/mL, respectively. In these figures, it can be observed perfectly how a simple increase of the solution concentration leads a great increase of mean particle size (PS) and particle size distribution (PSD).

Moreover, the same behaviour is reported in Fig. 4a and b. The curves of the lognormal distribution for each particle size distribution obtained from the experiments performed at different concentrations are shown in Fig. 4a. The mean particle sizes and standard deviations (S.D.) that characterize each particle size distribution are represented as points and vertical bars, respectively in Fig. 4b.

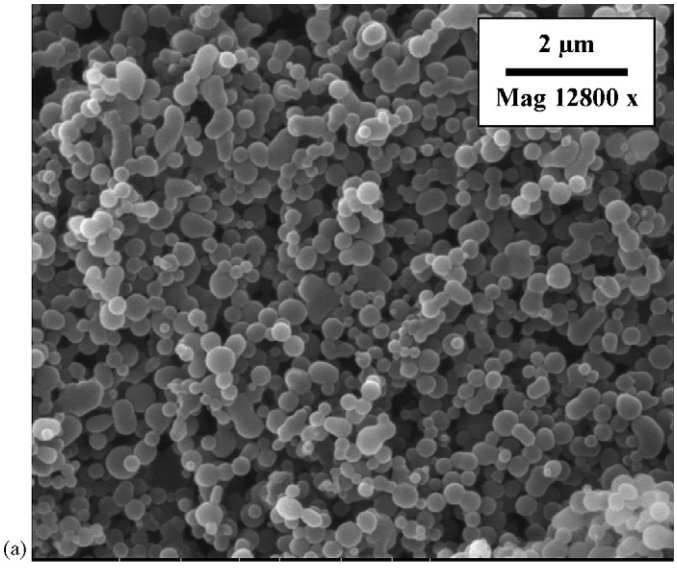

Fig. 3. Amoxicillin microparticles precipitated using two concentrations of the AMC–NMP solution equal to 20 mg/mL (a) and 100 mg/mL (b), respectively.

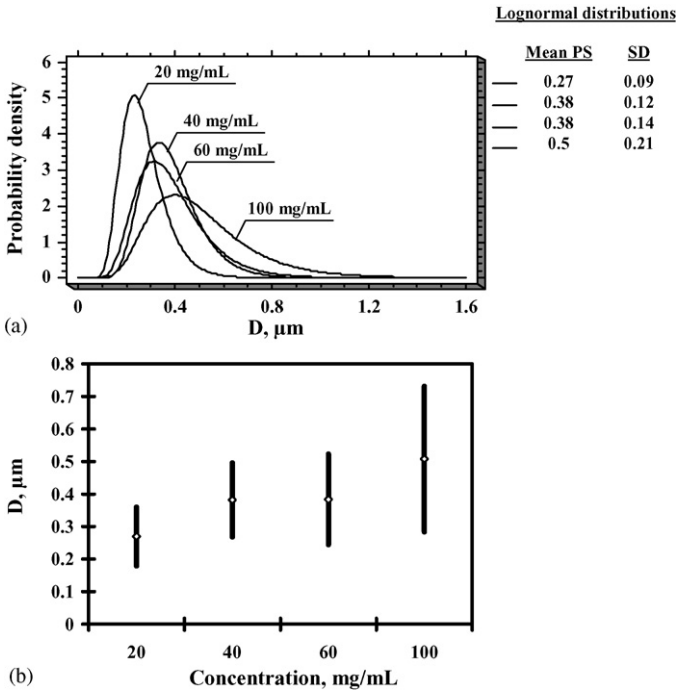

Fig. 4. Effect of the starting concentration of amoxicillin solution in NMP on particle size and particle size distribution. (a) Curves of the probability density function for each particle size distribution. (b) The mean PS and S.D. of each particle size distribution are reported as points and vertical bars, respectively.

Not only does the trend of our results agree with those obtained by Reverchon et al. [14], but we have also obtained smaller particle sizes than those obtained by those authors. This demonstrates that the process arrangement and the apparatus strongly influence the final product properties, as mentioned by Reverchon et al. [36] and that our equipment is very suitable for performing antibiotic precipitation processes using the SAS technique.

3. Results and discussion

One very important issue for the successful production of a precipitate by the SAS process is the chemical nature of the liquid solvent used for precipitation. Therefore, it was decided first to study which of the liquid solvents is most suitable for the controlled precipitation of ampicillin. Previously, Reverchon and Della Porta have attempted to precipitate ampicillin by the SAS technique using several different liquid solvents, but they were unable to obtain a successful precipitation of ampicillin and only reported the morphology of particles obtained at the bottom of precipitator vessel for the APC–DMSO system as a tight network [5].

Taking that attempt as our starting point we investigated the controlled precipitation of ampicillin using three differ-

ent solvents frequently used in research on antibiotic precipitation by the SAS technique [4,5,19]: *N*-methylpyrrolidone (NMP), dimethylsulfoxide (DMSO), and ethyl alcohol (EtOH). Experimental conditions (150 bar, 313 K, 20 mg/mL and ratio of CO_2 flow rate/liquid flow rate equal to 15, on a mass basis at the process operating conditions) were kept constant throughout the course of this investigation. Moreover, such conditions will assure us that we work well above the complete volume expansion for each liquid solvent tested [5].

First, we began studying the precipitation process for the APC–DMSO system. The test has been carried out according to the experimental procedures described previously. At the end of experiment, a film of the precipitated material with a porous appearance and a high content of solvent were obtained at the bottom of the precipitator vessel. The same result was obtained by Reverchon and Della Porta [5]. Regarding all the four basic phase behaviours suggested by Reverchon et al. [36], we think that an L-type mixture is formed in the precipitator vessel. The precipitation only took place in the rich liquid phase and no precipitation was observed from the upper fluid phase. That means a low partitioning of the solute between the two phases at 150 bar and 313 K.

Although APC is present at low concentration (initial concentration of the solution = 1.8 wt.%), our results can not be explained by the tentative pseudo binary vapour–liquid equilibrium diagram of the DMSO/CO_2 system in the presence of a solute at low concentration proposed by Reverchon et al. [36], since our operating point would be located well above the critical point of the mixture $MCP_{313\,K} \approx 95$ bar in the gas-rich side ($X_{CO_2} = 0.95$) where a homogeneous supercritical phase would have been formed.

During the course of the SAS process applied to the APC–EtOH system, a compact solid with a certain porous appearance was formed at the bottom of the precipitator vessel. Microparticles of ampicillin of both spherical and irregular shape with a mean diameter of 1.35 μm and standard deviation of 0.47 μm embedded within a network of interconnecting nanowires (mean diameter = 50 nm) have been observed. Fig. 5 shows a SEM image where examples of this morphology of ampicillin particles can be seen.

Thus, we think that this system has the same behaviour as the previous one, so an L-type mixture is found where precipitation only occurs in the rich liquid phase. If we consider the high-pressure vapour–liquid equilibrium diagram of the EtOH/CO_2 binary system [37], our operating point would be located well above the critical point of the mixture $MCP_{313\,K} \approx 80$ bar in the gas-rich side ($X_{CO_2} = 0.95$) where a homogeneous supercritical phase would have been formed.

Finally, when we used NMP as liquid solvent the behaviour observed was a process of substantial precipitation, in which the entire wall of the precipitator vessel was covered by a fine powder and a compact solid material impregnated with solvent was found in the frit. The SEM image of such powder shows the formation of spherical nanoparticles with a mean diameter = 0.26 μm, uniformly distributed, standard deviation = 0.08 μm as reported in Fig. 6.

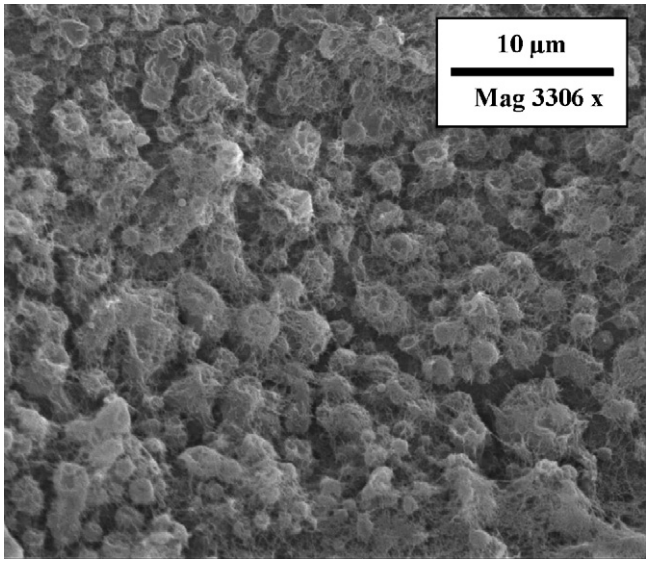

Fig. 5. SEM image of ampicillin microparticles precipitated from EtOH at 150 bar, 313 K, 20 mg/mL. Spherical and non-spherical microparticles can be recognized with a network of interconnecting nanowires.

We think that the L-type mixture is formed in the vessel and the precipitation took place from two phases due to the partition of the solute between these two phases at 150 bar and 313 K [36].

Rajasingam et al. [38] have presented experimental data on the solubility of CO_2 in DMSO and NMP at three temperatures from 298 to 318 K and at pressures approaching the mixture critical point for each binary system. At each temperature, the *P–x* curve for NMP lies below that for DMSO over the whole range of pressures considered (10–70 bar). This suggests that the $MCP_{313\,K}$ for NMP/CO_2 occurs below $MCP_{313\,K}$ for DMSO/CO_2 (≈95 bar) so our operating point would be

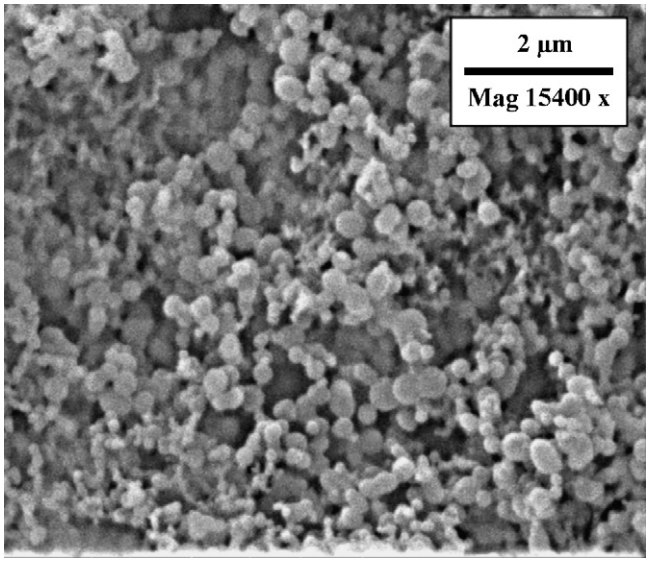

Fig. 6. SEM image of ampicillin nanoparticles precipitated from NMP at 150 bar, 313 K, 20 mg/mL.

located well above the mixture critical point in the gas-rich side ($X_{CO_2} = 0.97$) where a homogeneous supercritical phase would have been formed.

Considering our assumptions, spherical nanoparticles were precipitated from a supercritical phase in the upper part of the precipitation vessel, whereas, the compact APC was precipitated from a liquid phase formed at the bottom of the precipitator vessel.

In the three studied cases, the behaviour of the solvent/CO_2 binary systems has been modified by the addition of the APC increasing the pressure at which the complete miscibility between solvent and supercritical CO_2 occurs. However, in order to confirm our reasoning, a visual observation of the phase behaviour during the course of the precipitation process (using a windowed vessel) would be necessary. In this way, the relationship between phase behaviour and particle morphology obtained could be established.

The particle size distribution for both, APC–EtOH and APC–NMP systems can be fitted to normal distributions which are compared in Fig. 7a. The normal distribution was the function with a higher goodness of fit for this experimental data. The mean particle sizes and standard deviations for both distributions are represented in Fig. 7b. Through simply changing the APC–liquid solvent system we observed large variations in mean particle sizes and particle size distributions.

The APC–NMP proved to be the best system for controlling the precipitation of ampicillin. Consequently, the NMP solvent was selected to investigate the influence of the operating pressure. This influence has been studied in different systems by other authors, who found it to be the main factor for producing micronic and nanometric particles [4,5,19]. In this case, the ampicillin was successfully processed in the range of 80–150 bar, under constant experimental conditions (313 K, 20 mg/mL and ratio of CO_2 flow rate/liquid flow rate equal to 15, on a mass basis at the process operating conditions). At 80 bar, we found a continuous film of APC deposited on the frit inside the precipitator and no antibiotic on the walls of the vessel. The same physical behaviour was observed for the precipitation of tetracycline in NMP performed by Reverchon and Della Porta at a pressure lower than 100 bar [5]. A SEM image of ampicillin microparticles at 80 bar is shown as Fig. 8, where semispherical microparticles with a high level of coalescence can be observed.

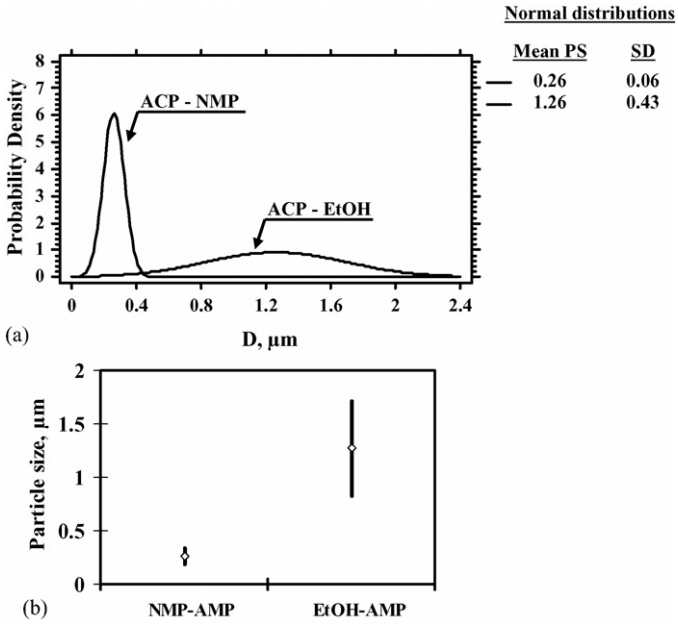

Fig. 7. Comparison of the particle size distributions for the systems: APC–NMP and APC–EtOH. (a) Probability density function for both systems. (b) The mean PS and S.D. of particle size distribution are reported as points and vertical bars, respectively.

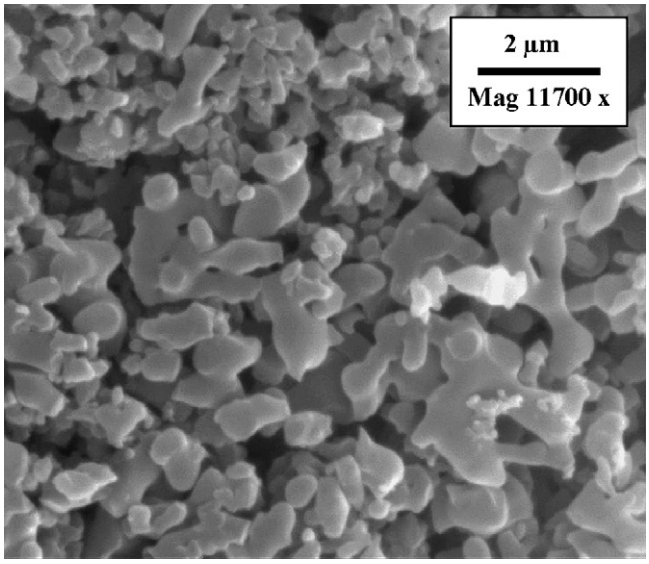

Fig. 8. SEM image of AMP microparticles precipitated at 80 bar.

Conversely, at greater pressures (>80 bar), APC was precipitated both like a fine powder on the walls and like solid aggregates in the frit of the precipitator vessel. An increase in pressure from 80 to 100 bar led to a great reduction of the mean PS and PSD. For pressures higher than 100 bar, the mean PS and PSD remained substantially unchanged until the highest pressure tested (150 bar). However, an enhancement in the sphericity of the particles and a decrease in their coalescence were observed. This behaviour is shown both qualitatively and quantitatively in Fig. 9a and 9b and in Fig. 10a and 10b, respectively.

Considering the change of behaviour of the NMP/CO_2 binary system in the presence of APC, we think that the L-type mixture is formed in the vessel at all pressure tested (80–150 bar). At 80 bar, the precipitation only occurred in the liquid-rich phase as a consequence of a low partitioning of the solute between the two phases at 80 bar and 313 K while at pressures higher than 100 bar, two phases are still formed but the solute partitioning also caused the precipitation in the upper fluid phase [36].

These results confirm that the increase of the operating pressure at constant temperature enhances the solvent power of supercritical CO_2 in respect of NMP; thus the liquid solvent molecules are more strongly captured by the antisolvent. Conversely, the possibility of interaction of APC with NMP is

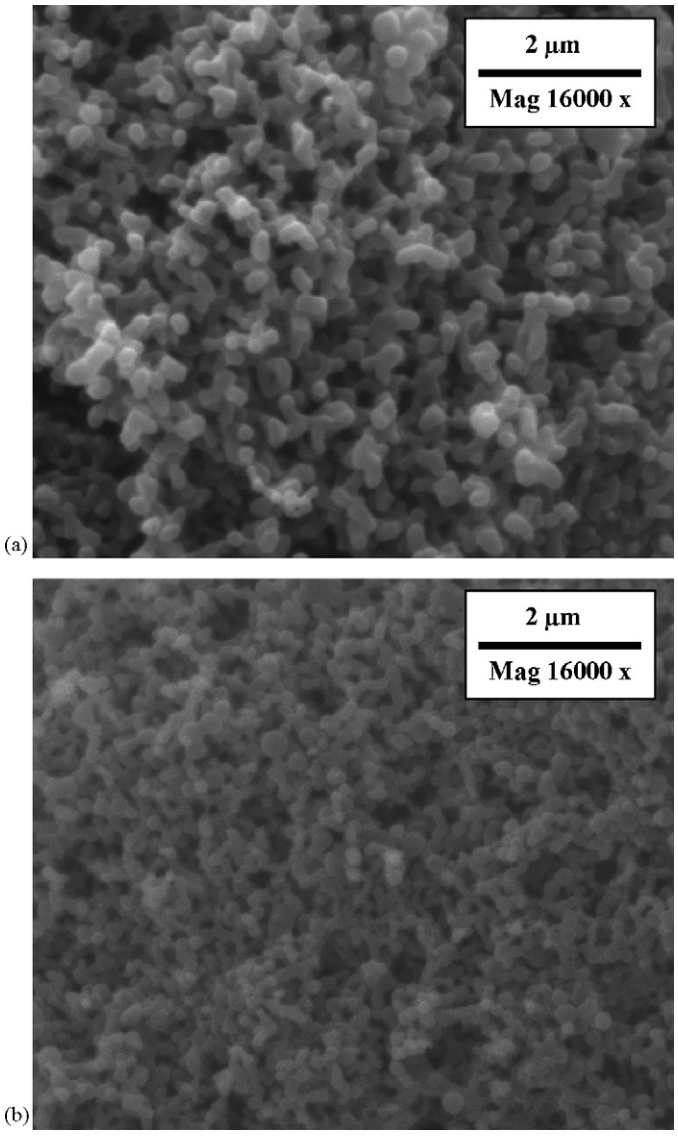

Fig. 9. SEM image at the same enlargement of ampicillin micronized from NMP at 20 mg/mL, 313 K and two pressures: (a) 125 bar and (b) 150 bar.

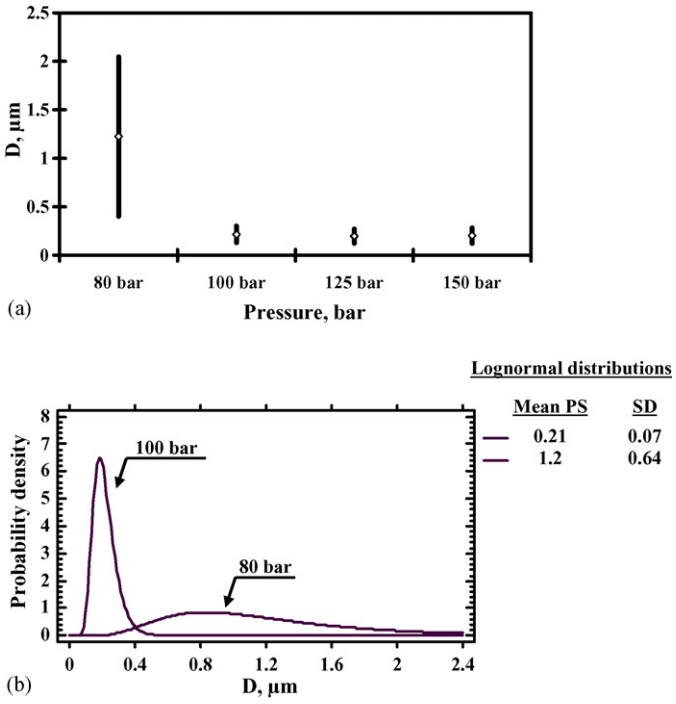

Fig. 10. (a) Variation of mean PS and PSD by altering the operating pressure. The mean PS and S.D. of particle size distribution are reported as points and vertical bars, respectively. (b) Probability density function for each particle size distribution obtained at two pressures (80 and 100 bar).

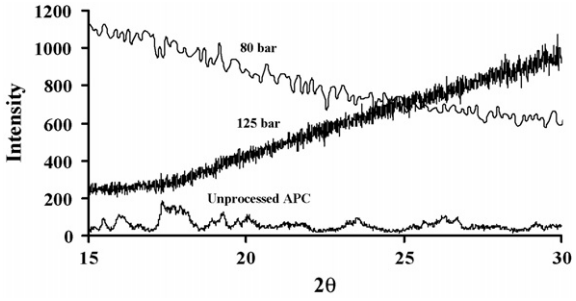

Fig. 11. Comparison of ampicillin XRD pattern before and after SAS processing.

reduced. This possible explanation was also given by Reverchon and Della Porta [5].

XRD patterns for samples of unprocessed ampicillin and ampicillin processed by SAS are compared in Fig. 11, where it can be seen how the ampicillin after the SAS process loses its crystalline structure since the main peaks of the unprocessed ampicillin disappear. This change from crystalline to amorphous structure has been observed in a few other cases of antibiotic precipitation by SAS and it has been attributed to the very fast precipitation that characterizes the SAS process, which does not allow time for the organization of the solute in crystalline form [5,14,19].

The amorphous solids have a great ability to absorb water vapour into its bulk structure forming an amorphous solution [39]. Therefore, the amorphous structure of ampicillin was also proved by its fast absorption of water vapour at high level of relatively humidity (RH%). A sudden formation of amorphous solution of ampicillin occurred above 60% of relatively humidity approximately.

4. Conclusions

SAS is a feasible process for the micronization of ampicillin. By simply changing the ampicillin–liquid solvent system we observed large variations in particle size and particle size distribution, accompanied with different particle morphologies. Three different solvents: *N*-methylpyrrolidone, dimethylsulfoxide, and ethyl alcohol have been used. When *N*-methylpyrrolidone was used, the precipitation was more successful compared with other solvents. It has been possible to produce nanometric ampicillin particles of mean particle diameter ranging from 0.1 to 0.3 μm with narrow particle size distributions. Moreover, the

spherical shape of particles and their coalescence can be controlled by varying the operating pressure. Ampicillin has been successfully processed in the range of 80–150 bar using *N*-methylpyrrolidone as liquid solvent under constant experimental conditions. A change from 80 to 100 bar led to a large reduction of the mean particle size and particle size distribution, but significant differences were not found at pressures higher than 100 bar.

This work is a preliminary study before undertaking a more in-depth study of the APC–NMP system precipitation by the SAS process. In fact, due to the large number of parameters involved in the SAS process, further experiments of the screening type will be undertaken to focus on the relative contribution of each parameter (i.e. pressure, temperature, concentration, nozzle, etc.) in determining the effects on particle size, particle size distribution and yield.

Acknowledgements

We are grateful to the INTERREG II-B program of the European Union and the Spanish Ministry of Science and Technology (project PPQ2003-04245) for financial support. We also wish to thank the Supercritical Fluid Center at UCC (University College Cork, Ireland) for their help.

References

[1] E. Reverchon, Supercritical antisolvent precipitation of micro- and nanoparticles, J. Supercrit. Fluids 15 (1999) 1.
[2] F. Dehghani, N.R. Foster, Dense gas anti-solvent processes for pharmaceutical formulation, Curr. Opin. Solid State Mater. Sci. 7 (2003) 363.
[3] G. Pifferi, A. Mannucci, Drug impurities: problems and regulations, Bollettino Chimico Farmaceutico 138 (1999) 500.
[4] E. Reverchon, G. Della Porta, P. Pallado, Supercritical antisolvent precipitation of salbutamol microparticles, Powder Technol. 114 (2001) 17.
[5] E. Reverchon, G. Della Porta, Production of antibiotic micro- and nanoparticles by supercritical antisolvent precipitation, Powder Technol. 106 (1999) 23.
[6] B.Y. Shekunov, P. York, Crystallization processes in pharmaceutical technology and drug delivery design, J. Cryst. Growth 211 (2000) 122.
[7] S.S. Dukhin, Y. Shen, R. Dave, R. Pfeffer, Droplet mass transfer, intradroplet nucleation and submicron particle production in two-phase flow of solvent-supercritical antisolvent emulsion, Colloid Surf. A: Physicochem. Eng. Aspect. 261 (2005) 163.
[8] H. Liu, N. Finn, M.Z. Yates, Encapsulation and sustained release of a model drug, indomethacin, using CO_2-based microencapsulation, Langmuir 21 (2005) 379.
[9] H. Tai, W. Wang, S.M. Howdle, Dispersion polymerization of vinylidene fluoride in supercritical carbon dioxide using a fluorinated graft maleic anhydride copolymer stabilizer, Macromolecules 38 (2005) 1542.
[10] Y. Wang, R. Pfeffer, R. Dave, R. Enick, Polymer encapsulation of fine particles by a supercritical antisolvent process, AIChE J. 51 (2005) 440.
[11] H. Steckel, B.W. Muller, Metered-dose inhaler formulation of fluticasone-17-propionate micronized with supercritical carbon dioxide using the alternative propellant HFA-227, Int. J. Pharm. 173 (1998) 25.
[12] J. Kerc, S. Srcic, Z. Knez, P. Sencar-Bozic, Micronization of drugs using supercritical carbon dioxide, Int. J. Pharm. 182 (1999) 33.
[13] M. Turk, P. Hils, B. Helfgen, K. Schaber, H.-J. Martin, M.A. Wahl, Micronization of pharmaceutical substances by the rapid expansion of supercritical solutions (RESS): a promising method to improve bioavailability of poorly soluble pharmaceutical agents, J. Supercrit. Fluids 22 (2002) 75.
[14] E. Reverchon, G. Della Porta, M.G. Falivene, Process parameters and morphology in amoxicillin micro and submicro particles generation by supercritical antisolvent precipitation, J. Supercrit. Fluids 17 (2000) 239.
[15] E. Reverchon, G. Della Porta, A. Spada, Ampicillin micronization by supercritical assisted atomization, J. Pharm. Pharmacol. 55 (2003) 1465.
[16] S. Moshashaee, M. Bisrat, R.T. Forbes, H. Nyqvist, P. York, Supercritical fluid processing of proteins I: lysozyme precipitation from organic solution, J. Pharmaceut. Sci. 11 (2000) 239.
[17] S. Bristow, T. Shekunov, B.Y. Shekunov, P. York, Analysis of the supersaturation and precipitation process with supercritical CO_2, J. Supercrit. Fluids 21 (2001) 257.
[18] S.P. Velaga, R. Ghaderi, J. Carlfors, Preparation and characterisation of hydrocortisone particles using a supercritical fluids extraction process, Int. J. Pharm. 231 (2002) 155.
[19] E. Reverchon, I. De Marco, G. Della Porta, Rifampicin microparticles production by supercritical antisolvent precipitation, Int. J. Pharm. 243 (2002) 83.
[20] P.M. Gosselin, R. Thibert, M. Preda, J.N. McMullen, Polymorphic properties of micronized carbamazepine produced by RESS, Int. J. Pharmaceut. 252 (2003) 225.
[21] T. Van Nijlen, G. Van Den Mooter, R. Kinget, P. Augustijns, N. Blaton, K. Brennan, Improvement of the dissolution rate of artemisinin by means of supercritical fluid technology and solid dispersions, Int. J. Pharmaceut. 254 (2003) 173.
[22] D. Kayrak, U. Akman, O. Hortacsu, Micronization of ibuprofen by RESS, J. Supercrit. Fluids 26 (2003) 17.
[23] E. Reverchon, G. Della Porta, Terbutaline microparticles suitable for aerosol delivery produced by supercritical assisted atomization, Int. J. Pharmaceut. 258 (2003) 1.
[24] S.D. Yeo, J.C. Lee, Crystallization of sulfarnethizole using the supercritical and liquid antisolvent processes, J. Supercrit. Fluids 30 (2004) 315.
[25] J.H. Kwon, C.W. Kim, A novel insulin microcrystals preparation using a seed zone method, J. Cryst. Growth 263 (2004) 536.
[26] S.P. Velaga, S. Bergh, J. Carlfors, Stability and aerodynamic behaviour of glucocorticoid particles prepared by a supercritical fluids process, Eur. J. Pharmaceut. Biopharmaceut. 21 (2004) 501.
[27] E. Reverchon, A. Spada, Erythromycin micro-particles produced by supercritical fluid atomization, Powder Technol. 141 (2004) 100.
[28] H. Steckel, L. Pichert, B.W. Müller, Influence of process parameters in the ASES process on particle properties of budesonide for pulmonary delivery, Eur. J. Pharmaceut. Biopharmaceut. 57 (2004) 507.
[29] M. Rehman, B.Y. Shekunov, P. York, D. Lechuga-Ballesteros, D.P. Miller, T. Tan, P. Colthorpe, Optimisation of powders for pulmonary delivery using supercritical fluid technology, Eur. J. Pharmaceut. Biopharmaceut. 22 (2004) 1.
[30] E. Reverchon, L. De Marco, Supercritical antisolvent micronization of Cefonicid: thermodynamic interpretation of results, J. Supercrit. Fluids 31 (2004) 207.
[31] C.-S. Su, Y.-P. Chen, Recrystallization of salicylamide using a batch supercritical antisolvent process, Chem. Eng. Technol. 28 (2005) 1177.
[32] P. Subra, A. Vega-González, C.-G. Laudani, E. Reverchon, Precipitation and phase behaviour of theophylline in solvent–supercritical CO_2 mixtures, J. Supercrit. Fluids 35 (2005) 95.
[33] S.P. Velaga, J. Carlfors, Supercritical fluids processing of recombinant human growth hormone, Drug Develop. Ind. Pharm. 31 (2005) 135.
[34] D.-H. Won, M.-S. Kim, S. Lee, J.-S. Park, S.-J. Hwang, Improved physicochemical characteristics of felodipine solid dispersion particles by supercritical anti-solvent precipitation process, Int. J. Pharmaceut. 301 (2005) 199.
[35] F. Miguel, A. Martín, M.J. Cocero, T. Gamse, Supercritical anti solvent precipitation of lycopene: effect of the operating parameters, J. Supercrit. Fluids 36 (2006) 225.

[36] E. Reverchon, G. Caputo, I. DeMarco, Role of phase behaviour and atomization in the supercritical antisolvent precipitation, Ind. Eng. Chem. Res. 42 (2003) 6406.

[37] S.N. Joung, C.W. Yoo, H.Y. Shin, S.Y. Kim, K.-P. Yoo, C.S. Lee, W.S. Huh, Measurements and correlation of high-pressure VLE of binary CO_2–alcohol systems (methanol, ethanol, 2-methoxyethanol and 2-ethoxyethanol), Fluid Phase Equilib. 185 (2001) 219.

[38] R. Rajasingam, L. Lioe, Q.T. Pham, F.P. Lucien, Solubility of carbon dioxide in dimethylsulfoxide and *N*-methyl-2-pyrrolidone at elevated pressure, J. Supercrit. Fluids 31 (2004) 227.

[39] G.Z. Evgenyi, Y. Shalaev, How does residual water affect the solid-state degradation of drugs in the amorphous state? J. Pharmaceut. Sci. 85 (1996) 1137.